

University of Nebraska - Lincoln

DigitalCommons@University of Nebraska - Lincoln

---

Mechanical & Materials Engineering Faculty  
Publications

Mechanical & Materials Engineering, Department  
of

---

2011

# Nanomechanical analysis of insulinoma cells after glucose and capsaicin stimulation using atomic force microscopy

Ruiguo Yang

*University of Nebraska-Lincoln, ryang6@unl.edu*

Ning Xi

*Michigan State University*

King Wai-chu Lai

*Michigan State University*

Bei-hua Zhong

*Michigan State University*

Carmen Kar-man Fung

*Michigan State University*

*See next page for additional authors*

Follow this and additional works at: <https://digitalcommons.unl.edu/mechengfacpub>

Part of the [Mechanics of Materials Commons](#), [Nanoscience and Nanotechnology Commons](#), [Other Engineering Science and Materials Commons](#), and the [Other Mechanical Engineering Commons](#)

---

Yang, Ruiguo; Xi, Ning; Lai, King Wai-chu; Zhong, Bei-hua; Fung, Carmen Kar-man; Qu, Chen-geng; and Wang, Donna H., "Nanomechanical analysis of insulinoma cells after glucose and capsaicin stimulation using atomic force microscopy" (2011).

*Mechanical & Materials Engineering Faculty Publications*. 367.

<https://digitalcommons.unl.edu/mechengfacpub/367>

This Article is brought to you for free and open access by the Mechanical & Materials Engineering, Department of at DigitalCommons@University of Nebraska - Lincoln. It has been accepted for inclusion in Mechanical & Materials Engineering Faculty Publications by an authorized administrator of DigitalCommons@University of Nebraska - Lincoln.

---

**Authors**

Ruiguo Yang, Ning Xi, King Wai-chu Lai, Bei-hua Zhong, Carmen Kar-man Fung, Chen-geng Qu, and Donna H. Wang



[Acta Pharmacol Sin.](#) 2011 Jun; 32(6): 853–860.

[Copyright](#) © 2011 CPS and SIMM

Received 2011 Mar 10; Accepted 2011 Apr 13.

Published online 2011 May 30. doi: [10.1038/aps.2011.56](https://doi.org/10.1038/aps.2011.56)

PMCID: PMC3852895

NIHMSID: [NIHMS528584](#)

PMID: [21623392](#)

<https://www.ncbi.nlm.nih.gov/pmc/articles/PMC3852895/?report=classic>

# **Nanomechanical analysis of insulinoma cells after glucose and capsaicin stimulation using atomic force microscopy**

Rui-guo Yang,<sup>1</sup> Ning Xi,<sup>1</sup> King Wai-chiu Lai,<sup>1</sup> Bei-hua Zhong,<sup>2,3</sup>  
Carmen Kar-man Fung,<sup>1</sup> Chen-geng Qu,<sup>1</sup> and Donna H Wang<sup>2,4,\*</sup>

<sup>1</sup>College of Engineering, Department of Electrical and Computer Engineering, Michigan State University, East Lansing, MI 48824, USA

<sup>2</sup>Department of Medicine, Michigan State University, East Lansing, MI 48824, USA

<sup>3</sup>Guangzhou Medical College, Guangzhou 510182 China

<sup>4</sup>Neuroscience Program, Cell and Molecular Biology Program, Michigan State University, USA

\*E-mail [ude.usm.ch@gnaw.annod](mailto:ude.usm.ch@gnaw.annod)

## **Abstract**

**Aim:** Glucose stimulates insulin secretion from pancreatic islet  $\beta$  cells by altering ion channel activity and membrane potential in the  $\beta$  cells. TRPV1 channel is expressed in the  $\beta$  cells and capsaicin induces insulin secretion similarly to glucose. This study aims to investigate the biophysical properties of the  $\beta$  cells upon stimulation of membrane channels using an atomic force microscopic (AFM) nanoindentation system.

**Methods:** ATCC insulinoma cell line was used. Cell stiffness, a marker of reorganization of cell membrane and cytoskeleton due to ion channel activation, was measured in real time using an integrated AFM nanoindentation system. Cell height that represented structural changes was simultaneously recorded along with cell stiffness.

**Results:** After administration of glucose (16, 20 and 40 mmol/L), the cell stiffness was markedly increased in a dose-dependent manner, whereas cell height was changed in an opposite way. Lower concentrations of capsaicin ( $1.67 \times 10^{-9}$  and  $1.67 \times 10^{-8}$  mol/L) increased the cell stiffness without altering cell height. In contrast, higher concentrations of capsaicin ( $1.67 \times 10^{-6}$  and  $1.67 \times 10^{-7}$  mol/L) had no effect on the cell physical properties.

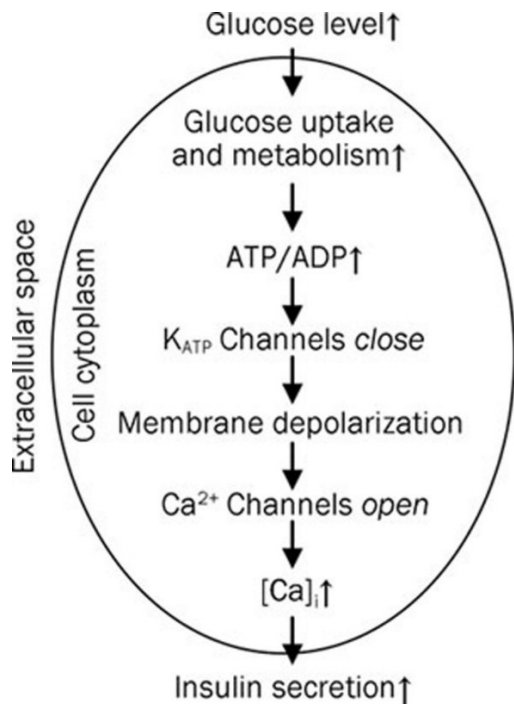
**Conclusion:** A unique bio-nanomechanical signature was identified for characterizing biophysical properties of insulinoma cells upon general or specific activation of membrane channels. This study may deepen our understanding of stimulus-secretion coupling of pancreatic islet cells that leads to insulin secretion.

**Keywords:** AFM nanoindentation, cellular stiffness, insulin secretion, glucose, capsaicin, cellular height

## Introduction

### Pancreatic $\beta$ -cell responses to glucose and capsaicin stimulation

Pancreatic  $\beta$ -cells are one of the main physiological units of the endocrine pancreas<sup>1</sup>, and they constitute about 65 to 90 percent of the islet cell population. Insulin, produced and released from pancreatic  $\beta$ -cells, is an important hormone that is involved in blood glucose homeostasis. In response to glucose stimulation, insulin is secreted from  $\beta$ -cells, a process known as stimulus-secretion coupling<sup>2</sup>. The resting potential of the  $\beta$ -cell membrane is determined primarily by the activity of ATP-dependent potassium channels ( $K_{ATP}$ ). When the plasma glucose level increases, glucose uptake and the  $\beta$ -cell metabolic rate will be enhanced, leading to the closure of  $K_{ATP}$  as the ATP/ADP ratio increases. As a result of the closure of  $K_{ATP}$ , the membrane potential changes, leading to the opening of voltage-gated calcium channels due to membrane depolarization. The increased cytoplasmic calcium concentration will ultimately result in insulin secretion ([Figure 1](#)). In addition,  $\beta$ -cell responses are synchronized with an oscillatory pattern, displaying pulse-like insulin secretion<sup>3</sup>.



[Open in a separate window](#)  
[Figure 1](#)

The stimulus-secretion coupling model of  $\beta$ -cells. Increased plasma glucose levels will increase the intracellular ATP/ADP ratio after glucose uptake by cells, which leads to the closure of ATP-dependent potassium channels, membrane depolarization, and the increase in intracellular  $\text{Ca}^{2+}$  concentrations that result in insulin secretion.

Capsaicin, the main ingredient of hot peppers, is a specific activator of the transient receptor potential vanilloid type 1 (TRPV1) channel, also known as the capsaicin receptor. Accumulating evidence showed that capsaicin-sensitive afferent nerves play a regulatory role in insulin secretion<sup>4</sup>. Studies also showed that activation of TRPV1 expressed in pancreatic islet  $\beta$  cells may modulate insulin secretion<sup>5</sup>. Despite the fact that capsaicin may activate TRPV1 leading to altered insulin secretion, the mechanisms underlying capsaicin mediated insulin secretion are largely unknown.

The electrophysiological properties of ion channels are important for cellular and organ function, and an ion channel defect in pancreatic islet  $\beta$  cells may lead to metabolic disorders. As such, these ion channels have been widely studied from various perspectives, most of which have made use of the patch-clamp technique to study the electrical activities of cells. While effective, the patch-clamp technique is very time consuming and demands highly skilled workers. Alternatively, other biophysical features may serve as biomarkers for assessing ion channel activities. Indeed, it has been shown that alterations in ion channel activity leading to insulin secretion would change the physical state of the cell membrane<sup>6</sup> and cytoskeleton<sup>7</sup>. Membrane bilayer stiffness depends on membrane protein configuration and deformation. The activation of ion channels can alter protein formation, the curvature of the membrane bilayer, and possibly the overall mechanical behavior of the cell<sup>8,9</sup>. Accordingly, this study was intended to develop a new technique to study the physical properties of pancreatic insulin secreting cells by characterizing

the nanomechanical properties of a single cell or cell population in order to identify unique biomarkers that respond to general or specific channel activators.

### **Mechanical property characterization using an atomic force microscopic (AFM) nanoindentation system**

AFM utilizes a cantilever with a sharp tip to probe the surface topography of various materials. AFM operates the cantilever to move across the sample surface in a raster scan. The fine scan motion was driven by a piezoelectric actuator with a high step resolution. During the scan, the interaction force between the scanning AFM tip and the sample surface bends the cantilever. A laser, which reflects back from the cantilever, records the deflection by readings of the laser spot position on a position sensitive device. The vertical movement of the piezoactuator, which keeps either the tip at a constant distance from the sample (contact mode) or the cantilever in constant oscillation amplitude (tapping mode), forms the topography image. The schematic drawing of the working principle of AFM is shown in [Figure 2A](#). AFM works perfectly well in liquid and makes measurements in real time, features that are ideal for biological applications and have unparalleled advantages over other high resolution imaging systems, including electron microscopy. Obtaining nanometer resolution images of cell membranes, DNA molecules and other biological structures has become possible with the recent development of AFM systems.

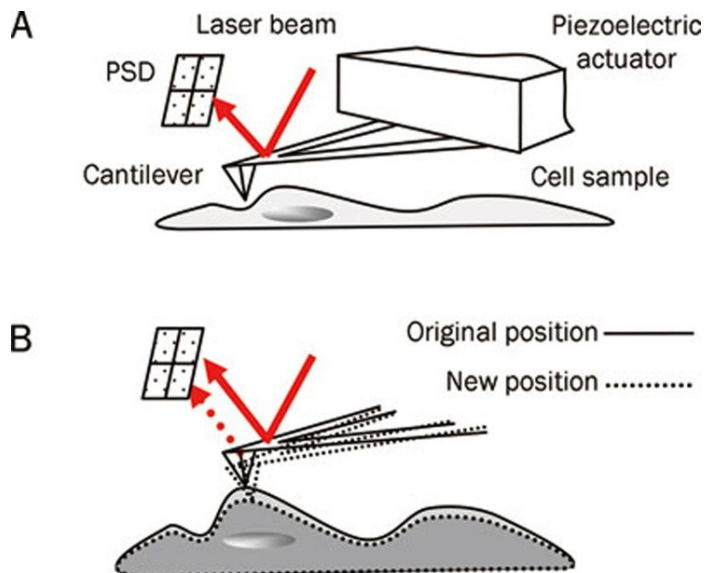


[Figure 2](#)

(A) AFM working principle. Briefly, the piezoelectric actuator drives the cantilever with a sharp tip at the end to perform a raster scan on sample surfaces. As it scans across the surface, the interaction force will bend the cantilever, and the bending is recorded by a laser reflected back from the cantilever. By maintaining the tip at a constant distance from the sample, a topography image is formed. (B) The initial contact point, indicated in [Figure 3](#) as a square, indicates the relative height of the sample. By recording the laser position of the contact point, the dynamic cell height can be obtained.

In addition to imaging, AFM is a natural nanoindenter, a feature that can be employed to probe the mechanical properties of materials. In nanoindentation mode, AFM drives a sharp tip into contact with the cell membrane and, consequently, deforms the membrane. By evaluating the indentation force and the indentation depth, the mechanical properties of the cell membrane may be obtained. The process will generate force-displacement curves as shown in [Figure 3](#). A Hertzian model is often used to fit the curve and to generate the Young's modulus value<sup>10</sup>.

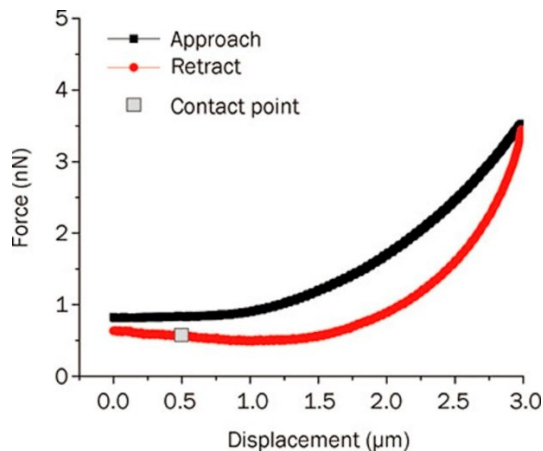


[Figure 3](#)

A typical force displacement curve with the contact point marked. The vertical motion will bring the AFM tip into contact with the cell and deform the cell (approach curve), followed by a retraction of the tip (retract curve). During the process, by recording the cantilever deflection (Y axis) with regard to the vertical displacement of the scanner (X axis), the force displacement curve is formed. The contact point is marked schematically as a square in the figure showing the point where the initial contact between the AFM tip and the sample is established.

When performing the force measurement on the same location of the cell, the AFM tip is drawn into contact by the interaction force (mainly van der Waals adhesive forces) between the tip and cell membrane. The contact point is indicated schematically by the square in the force curve shown in [Figure 3](#). When there are changes in the sample height, the contact point in the following force-displacement curves will correspondingly change in position as indicated by the laser spot ([Figure 2B](#)). Therefore, the relative cell height can be obtained by the continuous recording of the contact point. Normally, the absolute cell height and volume are measured by a topographical image, and it takes approximately 15 min to capture a single image. Given that the change in response to glucose stimulation happens rapidly, we considered the contact point measurement to be a faster method for monitoring height change.

### **AFM for the study of $\beta$ cell ion channel activities**

AFM has been applied to study biomarkers for a number of biological events<sup>11, 12, 13</sup>. In these events, changes in physiological conditions led to the reconfiguration of cell membranes and cytoskeleton structures. Cells exhibited distinct mechanical properties, including stiffness and viscosity, due to an altered cellular structure. Thus, AFM-based high resolution imaging and high

sensitivity force measurements for characterizing structural and mechanical biomarkers are feasible. For example, AFM has been used for the dynamic observation of mechanical property changes during the loss of cellular adhesion and apoptosis<sup>13</sup>. Using a similar strategy, this study aims to observe the physical changes of cell membranes in response to glucose and capsaicin stimulation in real time. The ability of AFM to record interaction forces and cell stiffness changes in the nanoscale in real time would provide a fresh perspective on these events.

## **Materials and methods**

### **Cell culture**

The insulinoma cells (ATCC, Manassas, VA, USA) were cultured to confluence in RPMI-1640 medium (Gibco-Invitrogen, Carlsbad, CA, USA) supplemented with 10% fetal calf serum and 1% penicillin and streptomycin at 37 °C in a humidified atmosphere containing 5% CO<sub>2</sub>. The cells were then seeded onto glass coverslips until reaching confluency.

### **Glucose stimulation**

Before each glucose stimulation experiment, the coverslips were placed in a petri dish with 5 mL of low glucose medium (2 mmol/L) for 90 min until equilibrium was reached. For glucose stimulation, volumes of 100 μL, 50 μL, or 40 μL of high glucose medium (2 mol/L) were added to the petri dish to make the final glucose concentrations 40 mmol/L, 20 mmol/L, or 16 mmol/L, respectively. A total of 100 μL of low glucose medium was added to a separate petri dish as a control.

### **Capsaicin stimulation**

Before each capsaicin stimulation experiment, the coverslips were placed in a petri dish containing 5 mL of Hanks' buffered salt solution (HBSS) for 90 min until equilibrium was reached. For capsaicin stimulation, 1 mL of HBSS medium with capsaicin concentrations of 10 nmol/L, 100 nmol/L, 1 μmol/L, and 10 μmol/L were added to the petri dish to obtain final concentrations of  $1.67 \times 10^{-9}$  mol/L,  $1.67 \times 10^{-8}$  mol/L,  $1.67 \times 10^{-7}$  mol/L, and  $1.67 \times 10^{-6}$  mol/L, respectively. HBSS 1 mL was added to a separate petri dish as control.

### **AFM measurements**

The insulinoma cells at equilibrium in the low glucose medium or HBSS were directly observed under the AFM equipped with an inverted microscope underneath. For statistical analysis, AFM nanoindentations were performed on 100 randomly selected cells before and after the stimulation. For the dynamic observation, 20 force displacement curves were taken as the baseline before the addition of glucose or capsaicin. After stimulation, force displacement curves were taken at a frequency of 1 Hz to dynamically monitor the stiffness change in real time for 1 h. To obtain higher sensitivity and to prevent the potential damage of the delicate cell membrane by the sharp AFM tip, the force applied to indent the cell was kept at a minimum. The maximum force applied was maintained below 10 nN, with the resulting deformation less than 100 nm, and



all force curves were taken at a loading rate of 1 Hz. Meanwhile, the contact point of the cantilever with the cell membrane was recorded to denote the relative cell height. [Figure 4](#) shows an optical image with the AFM cantilever above a single insulinoma cell before the force measurement.

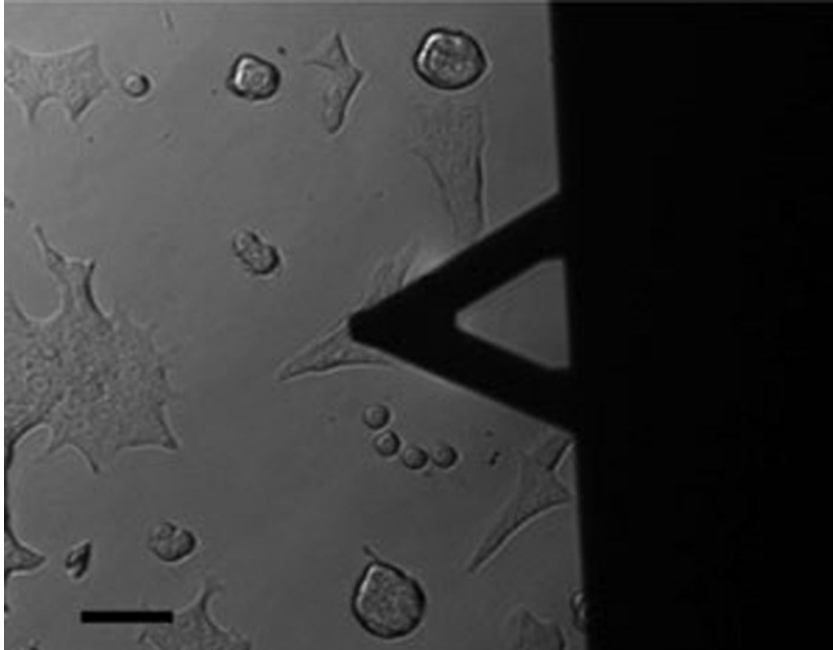


[Figure 4](#)

Optical image of an AFM cantilever above an insulinoma cell for nanomechanical property measurement obtained by an inverted optical microscope below the AFM. Scale bar: 50  $\mu\text{m}$ .

### **Force displacement curve processing**

In the AFM nanoindentation experiment, a conically shaped AFM tip with a silicon nitride cantilever (Bruker-nano, Santa Barbara, CA, USA) was used. The spring constant, which was 0.06 N/m, was calibrated using the thermal tune method. The applied force can be calculated by Hooke's law where:  $F=kd$ , where  $d$  is the deflection of the cantilever and  $k$  is the spring constant of the cantilever. According to the Hertzian model, for a conical shaped tip, the relationship between indentation and deformation is defined as:

$$F = \frac{2}{\pi} \frac{E}{1-\nu^2} \delta^2 \tan \alpha$$

where  $\alpha$  is the half angle of the cone-shaped tip,  $\nu$  is the Poisson ratio,  $F$  is the applied force,  $\delta$  is the indentation depth and  $E$  is the Young's modulus value. Young's moduli can be generated by fitting a force displacement curve. The half open angle of the tip is  $17.5^\circ$  and we used 0.5 as the Poisson ratio. A Matlab routine was developed to automate the calculation process.

# Results

## Glucose stimulation and stiffness measurement

For elasticity measurements, the Young's moduli calculated from the first 20 force curves before switching to high glucose were averaged as the baseline. The moduli from the first 20 min of measurements after the addition of high glucose medium were averaged as the positive results. As shown in [Figure 5A](#), the normal Young's modulus value for insulinoma in low glucose medium was around 7.0 kPa. The addition of high glucose medium increased the cell stiffness, and the increase displayed a dose-dependent pattern. The modulus increase resulting from the 40 mmol/L glucose stimulation was more than one fold, reaching 14.8 kPa. The 16 mmol/L glucose stimulation increased the stiffness to 13.9 kPa, while the 20 mmol/L glucose stimulation increased the stiffness to 14.2 kPa. The control showed no significant changes in stiffness in response to low glucose stimulation.

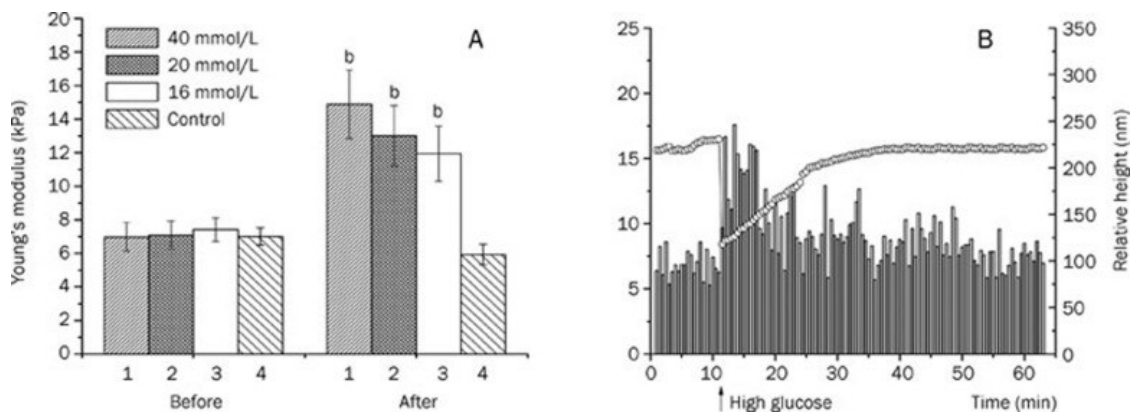


[Figure 5](#)

(A) The change in stiffness before and after administration of three different glucose levels: 16, 20, and 40 mmol/L, plus the control. Each datum was expressed as mean $\pm$ SEM. <sup>b</sup> $P < 0.05$  for 40, 20, and 16 mmol/L vs the control ( $n=20$ ). (B) Dynamic stiffness (bar) and cell height change (point scatters) after 20 mmol/L glucose stimulation.

For the relative height capture, dynamic monitoring showed that there was a sharp decrease in cell height around 120 nm at the onset of stimulation as indicated by the point scatter in [Figure 5B](#). The decrease of cell height was accompanied by the sharp increase of stiffness as shown in [Figure 5B](#). The addition of high glucose medium occurred at 11 min, and the final glucose level was 20 mmol/L. As the experiment continued, the cell height gradually recovered, and the stiffness gradually decreased. [Figure 6](#) shows the relationship between glucose concentration and cell height and stiffness, demonstrating that the increase in glucose concentration causes substantial changes in cell height and increases cell stiffness.

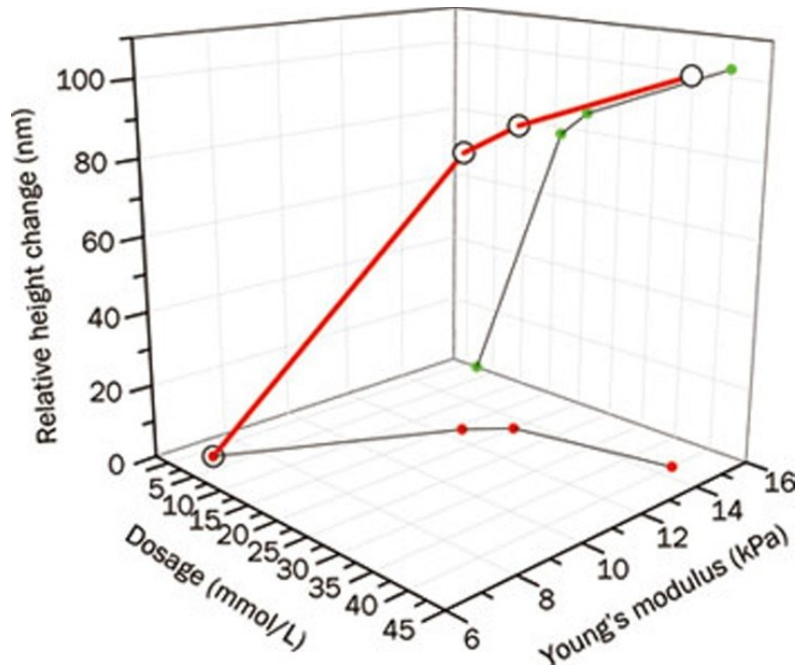


[Figure 6](#)

Glucose dosage is related to Young's modulus and change in cell height, with projections on each plane (bottom plane, stiffness vs dosage; right plane, height change vs dosage). There is a substantial increase in both height and stiffness in response to the glucose dosages of 16, 20, and 40 mmol/L compared to the baseline glucose concentration of 2 mmol/L.

## Capsaicin stimulation and stiffness measurement

### Nanomechanical property measurement of cell population

The capsaicin stimulation experiment was carried out in a similar fashion as the glucose stimulation experiment. However, unlike the glucose experiment, changes in stiffness after capsaicin stimulation were absent in some cells because they did not respond to capsaicin. Thus, we adopted a statistical approach by measuring the nanomechanical properties of a cell population from which the general cell property might be drawn. This approach has been used by a number of nanomedicine related studies<sup>12, 14</sup>. A total of 100 randomly selected cells were used prior to stimulation for baseline measurements. Thirty minutes after the addition of capsaicin, measurements were made on the same number of cells. Dose-dependent experiments of capsaicin were performed in the same fashion as in the glucose studies, and capsaicin was added in the following concentrations:  $1.67 \times 10^{-9}$ ,  $1.67 \times 10^{-8}$ ,  $1.67 \times 10^{-7}$  and  $1.67 \times 10^{-6}$  mol/L. Note that the Young's moduli of the insulinoma cell population has a normal distribution with one peak value (population mean) around 7.0 kPa, as indicated above. The dose studies showed that  $1.67 \times 10^{-9}$  mol/L, and  $1.67 \times 10^{-8}$  mol/L capsaicin caused changes in the physical properties of the cell population. The change was displayed as the change in peak percentile and the emergence of another peak at a higher Young's modulus value in the cell population ([Figure 7A3 and 7A4](#)), indicating that stiffness was increased in a portion of the cell population after stimulation. Thus, based on the responses, two groups had been identified: cells incapable of responding to

capsaicin stimulation sitting in the lower stiffness value peak and cells with responses to capsaicin stimulation residing in the higher stiffness value peak. In contrast, higher concentrations of capsaicin ( $1.67 \times 10^{-7}$  and  $1.67 \times 10^{-6}$  mol/L) had no effect on the cell physical properties as shown by the histogram in [Figure 7A1 and 7A2](#). The dose-dependent experiments were summarized in the cumulative distribution in [Figure 7B](#) with the horizontal line indicating the 50th percentile. As shown in [Figure 7](#), there was a clear stiffness shift at the 50th percentile line for  $1.67 \times 10^{-9}$  mol/L and  $1.67 \times 10^{-8}$  mol/L capsaicin stimulation compared to the unstimulated cells and the control. This was also confirmed by performing the mean value and deviation analysis as shown in [Figure 7C](#).

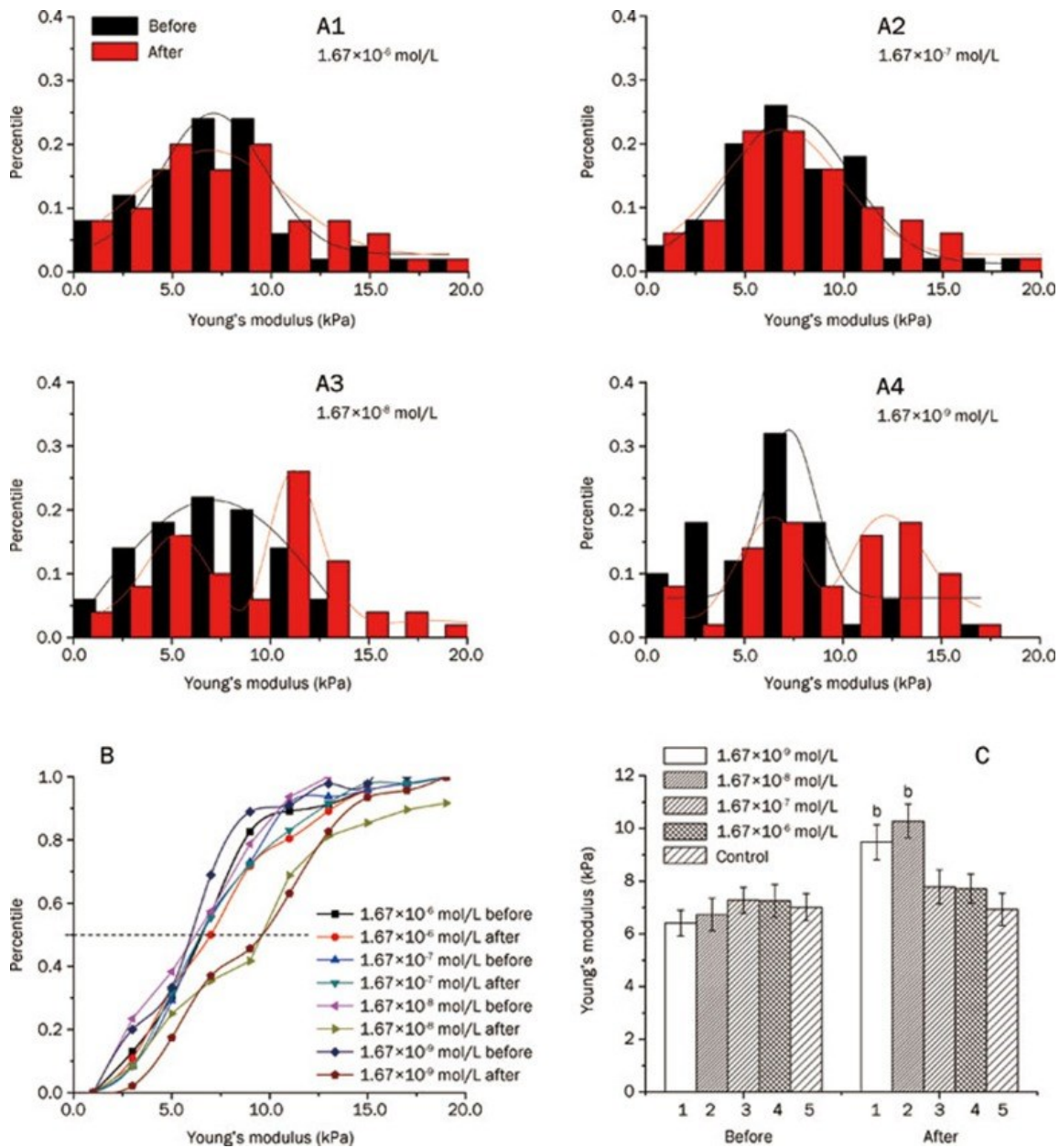


[Figure 7](#)

(A) Dose-dependent experimental results obtained from four different capsaicin concentrations: A1:  $1.67 \times 10^{-6}$  mol/L, A2:  $1.67 \times 10^{-7}$  mol/L, A3:  $1.67 \times 10^{-8}$  mol/L, and A4:  $1.67 \times 10^{-9}$  mol/L. (B) Summarized dose-dependent experiment with cumulative histogram. (C) Mean comparison of different doses with  $^bP < 0.05$  for  $1.67 \times 10^{-9}$  mol/L and  $1.67 \times 10^{-8}$  mol/L vs the control and  $^bP < 0.05$  for  $1.67 \times 10^{-9}$  mol/L and  $1.67 \times 10^{-8}$  mol/L vs  $1.67 \times 10^{-6}$  mol/L and  $1.67 \times 10^{-7}$  mol/L, respectively. Each datum is expressed as the mean  $\pm$  SEM ( $n=100$ ).

### Dynamic observation of stiffness and cell height after stimulation

The dose-dependent statistical analysis indicated that subgroups in the cell population responded differently to capsaicin stimulation. We next aimed to define the dynamic changes of cellular nanomechanical properties. A single cell was observed through the whole stimulation process with continuous measurement. This time-lapse experiment was similar to the glucose stimulation experiment for monitoring dynamic stiffness changes and height changes. The stimulation was carried out with  $1.67 \times 10^{-9}$  mol/L capsaicin that was added at 21 min. Before the addition of capsaicin buffer, the cell was observed for 20 min to obtain a baseline. The stiffening effect was not observed immediately following the stimulation, but it occurred about 10 min after capsaicin administration (Figure 8, bar). The cell Young's modulus increased from 7.0 kPa to 11 kPa and was maintained at this value throughout the experiment. However, the stiffening effect of capsaicin was not accompanied by a change in cell height (Figure 8, point scatters), as an overlaid point scatter plot indicated that the cell maintained the same height during the experiment.

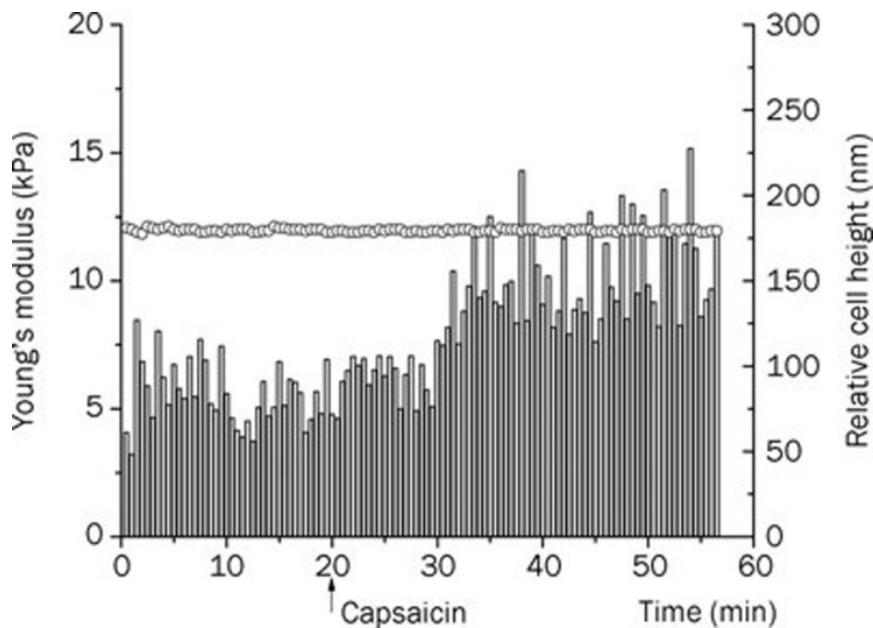


[Figure 8](#)

Dynamic stiffness (bar) and cell height change (point scatter) after  $1.67 \times 10^{-9}$  mol/L capsaicin stimulation.



Given the inhomogeneous nature of a cell body where different sites of a cell may respond differently to the applied indentation force, we wanted to ensure that inhomogeneity per se would not overshadow the true physiological state of the cell. To reach this goal, each cell was examined at three different locations on the membrane as depicted in [Figure 9](#): at the nucleus located at center of the cell, at the midpoint between the center and boundary of the cell, and at the boundary of the cell. Cells were examined in this fashion, and the results were plotted along with the mean of three measurements ([Figure 10A](#)). The mean value of the three measurements for each cell was then plotted in a histogram ([Figure 10B](#)) displaying a normal distribution with the peak value at 7.0 kPa, which is consistent with previous observations.

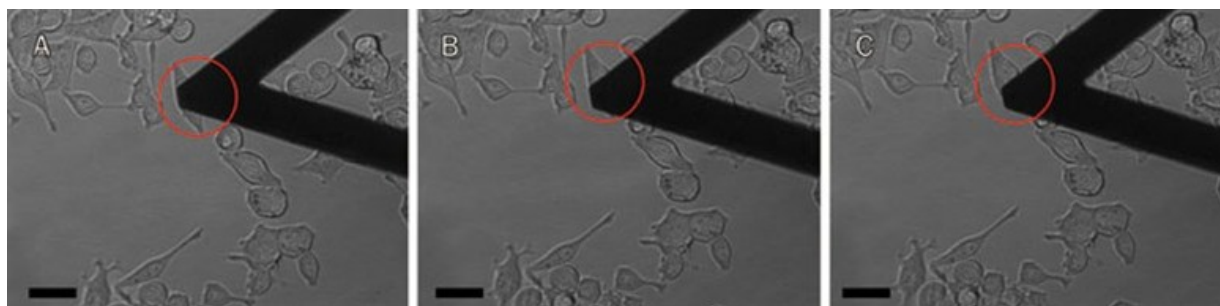


[Figure 9](#)

Position of measurement with AFM tip on top of an insulinoma cell: (A) nucleus; (B) middle between nucleus and boundary; and (C) boundary. Scale bar: 20  $\mu\text{m}$ .

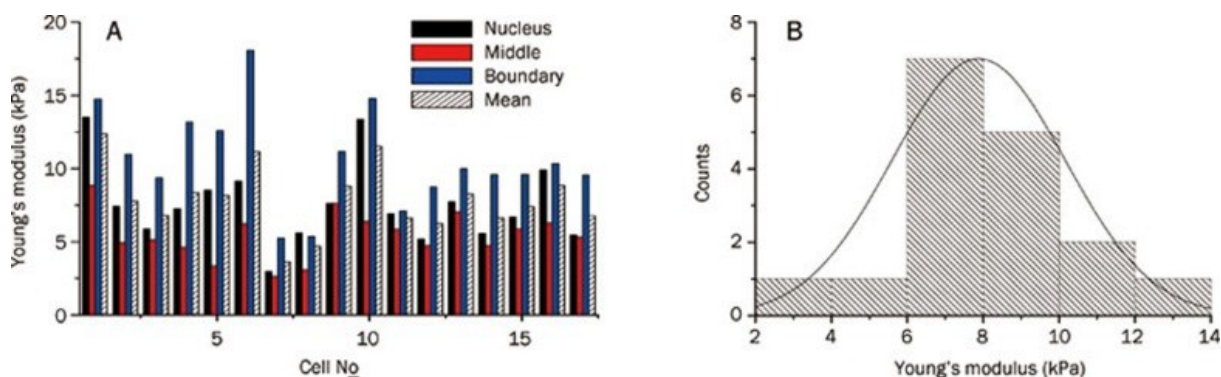


[Figure 10](#)

Measurement results on 17 cells at three different locations for each cell. (A) The mean of the three values for each cell, and (B) the distribution of the mean value with the peak at a similar value as previously established.

## Discussion

As elucidated in [Figure 1](#), it is known that increased glucose concentrations lead to changes in membrane potential and insulin secretion through glucose uptake<sup>15</sup>. The process is known as stimulus-secretion coupling<sup>2, 16, 17</sup>. With nanomechanical analysis, the results from the present

study show for the first time that cell stiffness increases in a dose-dependent manner in insulinoma cells subjected to glucose stimulation. In addition, cell height decreases with increased glucose concentrations in a synchronized fashion with stiffness changes as revealed by real time AFM nanoindentation measurements. Moreover, capsaicin has been shown to induce insulin secretion either via capsaicin-sensitive afferent neuron-mediated effects<sup>4</sup> or through activation of TRPV1 expressed in pancreatic islet  $\beta$  cells<sup>5, 18</sup>. AFM nanomechanical analysis of capsaicin stimulation in the present study reveals a distinct pattern of stiffness changes and dose-dependent effects from glucose stimulation; capsaicin at low ( $10^{-9}$  mol/L and  $10^{-8}$  mol/L), but not high, concentrations was able to increase stiffness without altering cellular heights in insulinoma cells.

Accumulating evidence has shown that altered ion channel activities occur and lead to insulin secretion<sup>17, 19, 20, 21</sup>. Altered ion channel activity may cause reorganization of the cellular membrane and cytoskeleton, resulting in changes of cellular stiffness<sup>6, 7, 8</sup>. Using an integrated AFM imaging system, we were able to measure cell stiffness and structural changes simultaneously upon stimulation of glucose and capsaicin (both known to alter ion channel activity and insulin secretion) on the nanoscale in real time. Distinct nanomechanical properties of insulinoma cell responses to glucose and capsaicin have been identified, which may indicate that a unique bio-nanomechanical signature is linked to a specific stimulus-secretion coupling of pancreatic islet cells that leads to insulin secretion.

Following glucose stimulation, we observed rapid decreases in cellular height. This physical change of cells may be explained by a number of glucose effects. In addition to altering ion channel activity, glucose may also change osmolarity, which may affect the configuration of the cellular structure. Before reaching equilibrium by glucose uptake, osmolarity outside of cells may be higher than that inside after glucose administration, which may lead to cellular shrinkage and contribute to increased cellular stiffness. Thus, increased cell stiffness after glucose administration may be attributed to altered ion channel activity and changes in osmolarity. In contrast, cells remain the same height in response to capsaicin administration, indicating that the shrinkage of cells due to altered osmolarity was absent in the capsaicin experiments. Moreover, cell stiffness increased only at low doses of capsaicin without altering cell height, further ruling out the possibility that concentrations of capsaicin may alter osmolarity and, therefore, cell stiffness. These results are consistent with a previous report where capsaicin induces insulin secretion only at low doses<sup>5</sup>.

The nature of small changes in cell stiffness presents a daunting challenge for detecting and capturing these changes. With the use of the AFM nanoindentation system, forces less than 10 nN can be applied, and the resulting changes in cell stiffness can be detected. Such a unique capability and the ultra-high sensitivity of the AFM nanoindentation system are indeed advantageous for studies focused on the cellular and molecule levels. Such an approach may provide insight into pancreatic  $\beta$ -cell stimulation secretion responses with a fresh perspective. With future development aimed at integrating AFM with traditional capabilities, including patch-clamp aptitude for measurement of ion channel activity and fluorescence optical microscopy assessment of intracellular  $\text{Ca}^{2+}$  concentrations, the next generation of the AFM system would indeed be a powerful tool to not only study pathophysiological events of ion channels and other molecules but also facilitate drug discovery.

**Author contribution:** Ning XI and Donna H WANG designed the research. Rui-guo YANG performed the experiments, analyzed the data and wrote the manuscript. Donna H WANG and King Wai-chiu LAI revised the paper. King Wai-chiu LAI, Bei-hua ZHONG, Carmen Kar-man FUNG, and Chen-geng QU assisted with the experiments.

**Acknowledgments:** This research was partially supported by NSF Grants IIS-0713346 and DMI-0500372, ONR Grants N00014-04-1-0799 and N00014-07-1-0935, NIH Grant R43 GM084520, HL-57853, HL-73287, and DK67620.

## References

1. Leung YM, Ahmed I, Sheu L, Tsushima RG, Diamant NE, Hara M, et al. Electrophysiological characterization of pancreatic islet cells in the mouse insulin promoter–green fluorescent protein mouse. *Endocrinology*. 2005;146:4766–75. [[PubMed](#)] [[Google Scholar](#)]
2. Juan-Pico P, Fuentes E, Bermudez-Silva FJ, Diaz-Molina FJ, Ripoll C, de Fonseca FR, et al. Cannabinoid receptors regulate  $\text{Ca}^{2+}$  signals and insulin secretion in pancreatic beta-cell. *Cell Calcium*. 2006;39:155–62. [[PubMed](#)] [[Google Scholar](#)]
3. Nilius B, Owsianik G, Voets T, Peters JA. Transient receptor potential cation channels in disease. *Physiol Rev*. 2007;87:165–217. [[PubMed](#)] [[Google Scholar](#)]
4. Karlsson S, Scheurink AJ, Steffens AB, Ahren B. Involvement of capsaicin-sensitive nerves in regulation of insulin secretion and glucose tolerance in conscious mice. *Am J Physiol*. 1994;267:R1071–7. [[PubMed](#)] [[Google Scholar](#)]
5. Akiba Y, Kato S, Katsube K, Nakamura M, Takeuchi K, Ishii H, et al. Transient receptor potential vanilloid subfamily 1 expressed in pancreatic islet beta cells modulates insulin secretion in rats. *Biochem Biophys Res Commun*. 2004;321:219–25. [[PubMed](#)] [[Google Scholar](#)]
6. Lundbaek JA, Birn P, Girshman J, Hansen AJ, Andersen OS. Membrane stiffness and channel function. *Biochemistry*. 1996;35:3825–30. [[PubMed](#)] [[Google Scholar](#)]
7. Cantiello HF. Role of the actin cytoskeleton on epithelial  $\text{Na}^+$  channel regulation. *Kidney Int*. 1995;48:970–84. [[PubMed](#)] [[Google Scholar](#)]
8. Lundbaek JA, Andersen OS. Spring constants for channel-induced lipid bilayer deformations estimates using gramicidin channels. *Biophys J*. 1999;76:889–95. [[PMC free article](#)] [[PubMed](#)] [[Google Scholar](#)]
9. Lim CT, Zhou EH, Quek ST. Mechanical models for living cells — A review. *J Biomech*. 2006;39:195–216. [[PubMed](#)] [[Google Scholar](#)]
10. Touhami A, Nysten B, Dufrene YF. Nanoscale mapping of the elasticity of microbial cells by atomic force microscopy. *Langmuir*. 2003;19:4539–43. [[Google Scholar](#)]
11. Pelling AE, Veraitch FS, Chu CP, Mason C, Horton MA. Mechanical dynamics of single cells during early apoptosis. *Cell Motil Cytoskeleton*. 2009;66:409–22. [[PubMed](#)] [[Google Scholar](#)]
12. Cross SE, Jin YS, Rao J, Gimzewski JK. Nanomechanical analysis of cells from cancer patients. *Nat Nanotechnol*. 2007;2:780–3. [[PubMed](#)] [[Google Scholar](#)]



13. Fung CKM, Seiffert-Sinha K, Lai KWC, Yang RG, Panyard D, Zhang JB, et al. Investigation of human keratinocyte cell adhesion using atomic force microscopy. *Nanomedicine*. 2010;6:191–200. [[PubMed](#)] [[Google Scholar](#)]
14. Hammerick KE, Huang Z, Sun N, Lam MT, Prinz FB, Wu JC, et al. Elastic properties of induced pluripotent stem cells. *Tissue Eng Part A*. 2011;17:495–502. [[PMC free article](#)] [[PubMed](#)] [[Google Scholar](#)]
15. Henquin JC. Triggering and amplifying pathways of regulation of insulin secretion by glucose. *Diabetes*. 2000;49:1751–60. [[PubMed](#)] [[Google Scholar](#)]
16. Malaisse WJ, Sener A, Koser M, Ravazzola M, Malaisse-Lagae F. The stimulus-secretion coupling of glucose-induced insulin release. Insulin release due to glycogenolysis in glucose-deprived islets. *Biochem J*. 1977;164:447–54. [[PMC free article](#)] [[PubMed](#)] [[Google Scholar](#)]
17. Henquin JC, Meissner HP. Significance of ionic fluxes and changes in membrane potential for stimulus-secretion coupling in pancreatic B-cells. *Experientia*. 1984;40:1043–52. [[PubMed](#)] [[Google Scholar](#)]
18. Schmidt PT, Tornøe K, Poulsen SS, Rasmussen TN, Holst JJ. Tachykinins in the porcine pancreas: potent exocrine and endocrine effects via NK-1 receptors. *Pancreas*. 2000;20:241–7. [[PubMed](#)] [[Google Scholar](#)]
19. Kilpatrick DL. Ion channels and membrane potential in stimulus-secretion coupling in adrenal paraneurons. *Can J Physiol Pharmacol*. 1984;62:477–83. [[PubMed](#)] [[Google Scholar](#)]
20. Ammala C, Kane C, Cosgrove KE, Chapman JC, Aynsley-Green A, Lindley KJ, et al. Characterization of ion channels in stimulus-secretion coupling in pancreatic islets. *Digestion*. 1997;58:81–5. [[PubMed](#)] [[Google Scholar](#)]
21. Petersen OH. Stimulus-secretion coupling: cytoplasmic calcium signals and the control of ion channels in exocrine acinar cells. *J Physiol*. 1992;448:1–51. [[PMC free article](#)] [[PubMed](#)] [[Google Scholar](#)]